In Vitro Self-Assembly of Proepicardial Cell Aggregates: An Embryonic Vasculogenic Model for Vascular Tissue Engineering

JOSÉ M. PÉREZ-POMARES,[1*] V. MIRONOV,[2] JUAN A. GUADIX,[1] DAVID MACÍAS,[1] ROGER R. MARKWALD,[2] AND RAMÓN MUÑOZ-CHÁPULI[1]

[1]Department of Animal Biology, Faculty of Science, University of Málaga, Málaga, Spain [2]Department of Cell Biology and Anatomy, Medical University of South Carolina, Charleston, South Carolina

ABSTRACT

Proepicardial/epicardial-derived cells are the main origin of the early embryonic coronary vascular bed. In vivo coronary vasculogenesis, which is a fast-occurring event, can be mimicked in vitro by culturing proepicardial tissue in different ways. The in vitro vasculogenic model presented in this study (a proepicardial suspension culture assay) partially reproduces coronary vascular development from its cellular precursors, a process known to be highly dependent on cell migration, cell differentiation, cell adhesion/sorting, and tissue fusion phenomena. The main aim of this study is to study the triggering signals and the cellular dynamics that regulate the differentiation of proepicardial cells into the angioblastic/endothelial lineage and their in vitro vasculogenic potential. Our results indicate that hanging drop-cultured proepicardia, which have an intrinsic vascular potential, behave like self-assembling cell aggregates or spheroids that can fuse to give rise to complex vascularized 3D structures. We believe that these self-assembling cell aggregates are an optimal choice to study the differentiation of coronary angioblasts, as well as a good method to reproduce vascular development in vitro. Finally, we propose the proepicardium as a suitable cellular source for vascular tissue engineering. Anat Rec Part A, 288A:700–713, 2006.

Key words: cell aggregates; cell fusion; proepicardium; coronary vasculogenesis; tissue engineering

Coronary vasculogenesis is an interesting kind of embryonic blood vessel formation. Cardiac vascularization takes place in a quite isolated environment (the pericardial cavity) and thus relatively far from common sources of vascular cell precursors. Although the cellular origin of coronary vessels has been under debate for many years (Männer et al., 2001; Wessels and Pérez-Pomares, 2004), recent findings have clearly shown that an important part of coronary cell types derives from the proepicardium and the epicardium (Mikawa and Fischman, 1992; Mikawa and Gourdie, 1996; Pérez-Pomares et al., 1998a, 1998b, 2002a, 2002b; Männer, 1999; Vrancken Peeters et al., 1999).

Origin and Differentiation of Coronary Cell Lineages

The proepicardium is the origin of the embryonic epicardium. Proepicardial cells derive from the coelomic epithelium and are mainly of epithelial nature. Proepicardial epithelial cells arrange themselves forming a system of protruding villi enclosing a well-hydrated extracellular matrix (the so-called proepicardial extracellular matrix), which confers to the proepicardium its characteristic cauliflower-like appearance (Männer et al., 2001). From their

*Correspondence to: José M. Pérez-Pomares, Department of Animal Biology, Faculty of Science, University of Málaga, Campus de Teatinos s/n, 29071 Málaga, Spain. Fax: 34-952-131-668. E-mail: jmperezp@uma.es

Received 26 August 2005; Accepted 28 February 2006

DOI 10.1002/ar.a.20338

Published online 7 June 2006 in Wiley InterScience (www.interscience.wiley.com).

original location at the caudalmost region of the embryonic tubular heart, proepicardial cells are transferred to the myocardial surface across the pericardial cavity to constitute the primitive epicardial epithelium. Both the epithelial components of the proepicardium and the epicardium (which represent two stages of a continuous morphogenetic process) undergo an epithelial-to-mesenchymal transformation (EMT), giving rise to a part of the mesenchymal cells found in the proepicardial extracellular matrix and to the majority of the subepicardial mesenchyme. This latter EMT-derived population of cells is also known as epicardially derived cells (EPDCs) (Gittenberger-de Groot et al., 1998; Pérez-Pomares et al., 2002b). These EPDCs contain the cellular progenitors of coronary vessels.

The development of the primary network of coronary blood vessels involves a tightly controlled differentiation of multiple cell types (endothelium, smooth muscle, and fibroblasts) from common cell progenitors (Mikawa and Fischman, 1992; Mikawa and Gourdie, 1996; Pérez-Pomares et al., 1998a, 1998b, 2002a, 2002b; Wessels and Pérez-Pomares, 2004). This differentiation is believed to be regulated by the myocardial secretion of growth factors, mainly fibroblast growth factors (FGFs) and vascular endothelial growth factor (VEGF) (Tomanek et al., 1999, 2001a, 2001b). However, it is not known whether the vasculogenic potential of proepicardial cells can be totally or partially triggered in vitro without the direct contribution of myocardial signals.

The differentiation of coronary precursor cells is linked to a series of events (cell adhesion, cell sorting, and tissue self-assembly or fusion), which are poorly studied in this system. As diverse cell types differentiate, the newly formed cellular populations establish contact, adhere or segregate in space based on their mutual affinity. These cellular phenomena, which constitute a key morphogenetic step, have not been carefully studied for coronary cell precursors either in vivo or in vitro, although several elegant studies using in vitro culture of embryonic cells and multiple cell lines have set an excellent conceptual and experimental frame to analyze these cellular mechanisms (Steinberg 1962a, 1962b, 1963; Foty et al., 1994, 1996; Foty and Steinberg, 2005). In the embryo, the final outcome of these processes is the development of structures of increasing complexity.

Morphogenesis: Acquiring a Third Dimension

The vertebrate embryo initially develops as a bidimensional structure. The first 3D structural elements developed by the early embryo are spheroids (massive or hollow) and tubes. It is well known that blood vessels, which are an excellent example of embryonic tube morphogenesis, can form by vasculogenesis [i.e., the coalescence of isolated mesenchymal progenitors called angioblasts (González-Crussi, 1971; Risau and Lemmon, 1988; Risau and Flamme, 1995)] or by angiogenesis [i.e., the growth from preexisting vessels (Hertig, 1935; Risau and Lemmon, 1988)]. Vasculogenesis is a paradigmatic kind of mesodermal tube formation (Hogan and Kolodziej, 2002) involving diverse cell types that will eventually arrange themselves into distinct concentric layers. The coalescence of angioblasts (acting as the primary vascular units or vascular pieces) to form endothelial vesicles and chords (which can be regarded as secondary vascular units or vascular domains) and the following fusion or self-assembly of these domains are pivotal to the complete formation of a vascular tube (reviewed in Risau and Flamme, 1995). In this regard, it is important to emphasize that coronary vasculogenesis takes place by the fusion of discrete vascular colonies (Mikawa and Fischman, 1992) to form an intricate but clearly patterned network of arteries, arterioles, veins, venules, and capillaries (Vrancken Peeters et al., 1997a, 1997b). Thus, part of the biological relevance of this morphogenetic mechanism relies on its ability to create blood vessels of diverse caliber from unicellular precursors (a singular feature that vasculogenesis does not share with angiogenesis) and its sensitivity to signals accounting for spatial vessel patterning. All these characteristics make embryonic vasculogenic phenomena important not only for the developmental biologist, but also for the tissue engineer.

Tissue Engineering and Developmental Biology

For more than a decade, tissue engineering technologies have focused on the controlled development of 3D cellular structures enabling the development of organs in vitro (Langer and Vacanti, 1993; Nerem and Sambanis, 1995). It is obvious that de novo-developed organs should perform as efficient complex living structures to substitute traditional surgical reconstruction and regular allogenic organ transplantation (as discussed by Vacanti and Langer, 1999). To maintain, improve, restore, or substitute human tissues is the ultimate goal of tissue engineering (Lalan et al., 2001). It is therefore easy to understand that tissue engineering necessarily finds in embryonic development the essential inspiration to attempt the growth of tissues and organs in vitro. A generally accepted principle is that tissue engineering must try to recapitulate regular ontogenetic processes to imitate the almost perfect developmental mechanisms assayed by nature throughout thousands of years (Lanza et al., 2000; Mironov et al., 2003). To learn, for each case, which ones are the necessary and sufficient elements that, in the proper combination, will lead to the development of a complex functional organ with a specific form is the biggest challenge for the tissue engineer. To accomplish this task in vitro, we have to define how cell diversity is achieved in a developing sophisticated multicellular structure, how cells interact between them and with the extracellular matrix (ECM), how cell-to-cell and cell-to-matrix interactions determine morphogenetic movements outlining a defined shape or form, and how the environment modulates the process.

Coronary Morphogenesis as a Model for Vascular Tissue Engineering

From the point of view of the tissue engineer, developing blood vessels in vitro is not only important because of the obvious clinical and surgical implications, but also because the proper vascularization of any engineered tissue or organ is crucial to its integrity and viability (Lanza et al., 2000).

Proepicardial cells display a unique in vivo vascular differentiation potential that has not yet been extensively tested in vitro. To study if proepicardial differentiation into coronary angioblasts can be achieved and modulated in vitro and to define the vasculogenic potential of these cells in our culture system are the main goals of the present work. It is important to indicate that although

other cell types are known to derive from the proepicardium (e.g., smooth muscle and fibroblastic cells) (Wessels and Pérez-Pomares, 2004), in this study we will only focus on the emergence of angioblastic/vascular endothelial cells, which seem to be the very first ones differentiating from proepicardial tissue (Pérez-Pomares et al., 2002a; Guadix et al., 2006). Furthermore, endothelial differentiation is known to influence smooth muscle differentiation directly, so we considered it was necessary to start analyzing the vascular endothelial aspect of proepicardial in vitro development.

In order to tackle the issue, we have applied the classic hanging drop culture system (Rudnicki and McBurney, 1987) to study coronary angioblastic differentiation and the morphogenetic dynamics of these cells. Hanging drop culture systems have already been used to study embryonic mesenchyme behavior (Armstrong and Armstrong, 2003) and cardiac muscle development (Armstrong et al., 2000), but have never been set to test morphogenetic properties of proepicardial cells, which are known to display pluripotent abilities. The main reason for choosing this culture system is that it helps to maintain a basic cell density in vitro, without the expected dispersion of cells in a cell-substrate attachment-dependent culture method. An additional aim of this study is to show that proepicardial aggregates can coalesce in vitro to form vascularized structures of diverse complexity. The formation and significance of these structures will be discussed from the perspective of both the developmental biologist and the tissue engineer.

MATERIALS AND METHODS

Isolation of Proepicardia and Embryonic Myocardium From Avian Embryos

The animals used in our research were handled in compliance with the international guidelines for animal care and welfare. Chick and quail eggs were kept in a rocking incubator at 38°C. The embryos were staged according to the Hamburger and Hamilton (1951) stages of chick development, excised, the extraembryonic membranes removed, and the embryos extensively washed in EBSS (Gibco). Sharp tungsten needles, small iridectomy forceps, and scissors were used to isolate quail proepicardia under a dissecting scope. Proepicardia from H/H16-17 quail embryos were stored in culture media (M199, 1% chick serum, penicillin/streptomycin) at 37°C, 5% CO_2, before trypsinization (5 min at 37°C in 0.25% trypsin-EDTA diluted in M199 from the 2.5% stock; Gibco) and/or definitive culture.

Extraction of chick embryonic myocardium from ventricular chambers was performed as follows. H/H16-17 ventricular sections of the heart tube were isolated and the explants cultured on 1.5 mg/ml drained rat tail type I collagen gels (Collaborative Research) with the endocardium facing the surface of the gel. After 3–4 hr of incubation at 37°C, 5% CO_2, the myocardium was mechanically separated from the endocardium, which remained attached to the gel. Myocardial tissue was routinely trypsinized for 5 min at 37°C in a 0.25% trypsin-EDTA solution in M199 (Gibco). Digestion was stopped with 10% FBS (Gibco) in M199 medium (Gibco). After centrifugation, the cells were resuspended in fresh M199 supplemented with 100 ng/ml bFGF (Peprotech), 1% chick serum (Sigma), and 100 IU penicillin/streptomycin (Gibco).

Culture of Cell Aggregates

The aggregation of cells and tissues to form cell spheroids/aggregates was performed in a hanging drop (20 μl) culture system (Rudnicki and McBurney, 1987) set in Petri dishes (35 mm of diameter). The cultures were monitored under a Leica DMLB scope and photographed using a Nikon DXM-1200 digital camera. For regular aggregation of quail proepicardial tissue into a single spheroid, two or three proepicardia were cultured together in fresh M199 medium supplemented with 100 ng/ml bFGF (Peprotech), 10 ng/ml VEGF (Peprotech), 1% chick serum (Sigma), and 100 IU penicillin/streptomycin (Gibco) for 12–18 hr (a preliminary test to define the growth factor concentrations used in our culture system was carried out using 50 ng/ml bFGF and 5 ng/ml VEGF). Rod-like structures were obtained by shaping the hanging drops as ovoidal ones. Growth factor concentrations were suggested by different studies dealing with the differentiation of early quail embryonic mesodermal cells into angioblasts (Krah et al., 1994; Eisenberg and Markwald, 1997). Preliminary assays to test different growth factor concentrations were also developed in our laboratory (see Results).

Control proepicardia were cultured without the growth factor supplement for 1 hr. To develop rod-like constructs, two, three, or four of these isolated proepicardial spheroids/aggregates were cultured again for 3–4 hr (total culture time, including the formation of the aggregates, was 16–22 hr) in the same experimental conditions. The ability of these cell aggregates to fuse spontaneously was also tested by culturing them for 3–4 hr on 1.5 mg/ml drained rat tail type I collagen gels (Collaborative Research). In some cases, quail and chick proepicardial aggregates were cocultured and assembled to test cell mixing and fusion dynamics. Before fusing them, CCFSE (5,6-carboxy-2′-7′-dichlorofluorescein diacetate succinimidyl ester; Molecular Probes) was used to stain the outer surface of chick proepicardial aggregates. Quail cells were routinely localized by QCPN or QH1 staining. In order to test the proepicardial potential to vascularize the myocardium in vitro, quail proepicardia were aggregated and cocultured with myocardial cells, giving rise to chimeric spheroids. Proepicardial-myocardial aggregation was carried out after trypsinization of the tissues (as stated above) and mixing 6,000–8,000 chick myocardial cells and 1,000–2,000 quail proepicardial cells per drop (20 μl). Cultures were incubated at 37°C, 5% CO_2, in M199 supplemented with 1% chick serum (Sigma) and 100 IU penicillin/streptomycin (Gibco) for 12–18 hr. For these chimeric aggregates, controls were made only of chick myocardial cells. Aggregates showing evident morphological signs of necrosis (around 5%) (De la Pompa and Zeller, 1993) were discarded for (immuno)histological purposes (i.e., analysis of lumen formation and development of vascular structures).

Scanning Electron Microscopy (SEM)

Quail embryos as well as single and fused cell spheroids were fixed in 1% paraformaldehyde-1% glutaraldehyde in PBS (1 hr), washed in PBS buffer, and postfixed in 1% OsO_4 for 30 min. After washing in bidistilled water, the embryos were dehydrated in an ethanolic series finishing in 100° ethanol and dried from liquid CO_2 by the critical-point method, whereas cell aggregates were air-dried. All the samples were gold-sputted (about 450 Å) in a JEOL

fine-coat ion sputter (JFC-1100), observed, and photographed in a JEOL JSM-840 scanning electron microscope operated between 10 and 20 kV. In some special cases, cell spheroids/aggregates were embedded in paraffin after OsO_4 postfixation and sectioned in a Leitz microtome to analyze the core of the structures. After exposing the desired area, the tissue was dewaxed in xylene, washed in 100° ethanol, and processed for the scanning microscope as described.

Semithin Sections

Proepicardial cell aggregates were fixed, postfixed, and dehydrated as described for SEM procedures. After an acetone transition step, the tissues were embedded in Araldite 502 (Fluka), and the samples polymerized at 60°C for a period of 3 days. Then, 0.5 μm sections were cut on an ultramicrotome (Reichert UMO-2), mounted on glass slides (Menzel-Gläser), and stained with toluidine blue.

Immunohistochemistry of Cell Aggregates

Before fixation, cell spheroids/aggregates were extensively washed in PBS. For whole mount immunohistochemistry, the tissue was fixed in 70% methanol on poly-L-lysinated (0.01%; Sigma) microscope slides (Menzel-Gläser), whereas for immunohistochemistry on tissue sections, cell aggregates were fixed in 4% paraformaldehyde, dehydrated in ethanol, cleared in butanol, embedded in Histosec (Merck), and 5 μm-sectioned in a Leitz microtome.

The monoclonal QCPN antibody is a quail pan-nuclear marker, whereas the QH1 antibody is a specific quail hemangioblastic marker (both purchased from the DSHB). The 5H6 is a monoclonal antibody developed against quail VEGFR-2 (Dr. A Eichmann) and the anti-L-CAM (avian E-cadherin) is a mouse monoclonal (DSHB). The MF20 monoclonal antibody (DSHB) and the L53 polyclonal (Dr. A.F. Moorman) antibodies were developed against myosin heavy chain epitopes. The anticytokeratin (CK) antibody is a wide screening rabbit polyclonal (Dako). The anti-RALDH2 antibody is a rabbit polyclonal (Drs. P. McCaffery and U. Drägger).

Briefly, samples were washed in Tris-PBS, and nonspecific binding sites were saturated for 30 min in 16% sheep serum, 1% bovine serum albumin, and 0.5% Triton X-100 in Tris-PBS (SBT). For single fluorescent labeling, the samples were incubated overnight at 4°C in the primary monoclonal antibodies (1:200 QH1 dilution in SBT, 1:15 MF20 dilution in SBT, pure QCPN, pure L-CAM). Incubation of the primary antibody was followed by an overnight incubation (4°C) in a secondary FITC-conjugated goat antimouse IgG (Sigma), a secondary TRITC-conjugated goat antimouse IgG (Sigma), or a secondary Cy5-conjugated donkey antimouse IgG (Jackson Laboratories), Tris-PBS washes, and optional propidium iodide nuclear counterstaining. Double fluorescent labeling of proepicardial chimeric aggregates was performed using a combination of polyclonal and monoclonal primary antibodies. The samples were incubated overnight at 4°C in the primary polyclonal antibody (L53 diluted 1:25 in SBT, anti-CK diluted 1:100 in SBT, anti-RALDH2 diluted 1:5,000 in SBT). Then the tissue was washed in Tris-PBS, incubated for 2 hr at room temperature in a Cy5-conjugated donkey antirabbit IgG (Jackson Laboratories) or a FITC-conjugated goat antirabbit IgG, washed in Tris-PBS, and incubated overnight at 4°C in the QH1 or the QCPN monoclonal antibodies (used at a 1:200 dilution in SBT or pure, respectively). After washing, the samples were incubated in a FITC-conjugated goat antimouse IgG or a Cy5-conjugated donkey antimouse IgG (2 hr, room temperature), washed again, mounted in a 1:1 PBS/glycerol solution, and analyzed using a Leica TCS/NT laser scanning confocal microscope. Negative controls were always performed incubating the sections with SBT instead of the primary antibody.

For VEGFR-2 immunohistochemistry, the cell aggregates were fixed in 4% paraformaldehyde, washed in PBS, and cryoprotected in 15% and 30% PBS sucrose solutions, where they were kept at 4°C until embedding. Then, the cell spheroids were immediately embedded in OCT-embedding media (TissueTek) and snap-frozen in liquid nitrogen-cooled isopentane. Sections (10 μm) were obtained in a cryostat (Reichert-Jung) and collected on poly-L-lysine-coated slides. Nonspecific binding sites were saturated for 30 min in SBT and the sections were incubated overnight in undiluted 5H6 hybridoma supernatant (4°C). Finally, the tyramide signal amplification system (Perkin Elmer) was applied following the indications provided by the suppliers (a biotin-conjugated antimouse IgG was used as a secondary antibody and FITC-coupled streptavidin was used as the fluorescent reporter).

TUNEL Assay

Proepicardial cell aggregates were fixed in 4% paraformaldehyde, dehydrated, sectioned, and mounted as described above. Sections were incubated in 10 μg/ml proteinase K in 10 mM Tris-HCl buffer (pH 7.4) for 30 min at 37°C. After extensive washes in PBS, the tissue was permeabilized in a 0.1% Triton X-100/0.1% sodium citrate solution in distilled water (2 min, 4°C) and washed again in PBS. The TUNEL method was used to detect in situ cell death following the manufacturer's instructions (Roche). Immunohistochemical detection of quail endothelial cells followed the TUNEL assay. Briefly, slides were washed in Tris-PBS and nonspecific binding sites were saturated for 30 min in 16% sheep serum, 1% bovine serum albumin, and 0.5% Triton X-100 in Tris-PBS (SBT). Then, the slides were incubated overnight at 4°C in a 1:200 dilution in SBT of the QH1 monoclonal antibody, washed in Tris-PBS, and incubated again (4°C) in a secondary Cy5-conjugated donkey antimouse IgG (Jackson Laboratories). After final Tris-PBS washes, the sections were mounted as indicated and analyzed under a laser scanning confocal microscope (Leica TCS-NT).

RESULTS

Culture and Analysis of External Morphology of Proepicardial Aggregates

Aggregation of two proepicardia formed spheroids of around 200 μm in diameter, whereas aggregation of three proepicardia led to the development of spheroids of an approximate diameter of 300 μm (Fig. 1A–F). Slight deformation of the cell aggregates to an ovoid conformation was frequent after fixation and embedding of the samples. An average of 8 hr was needed to make the proepicardia to

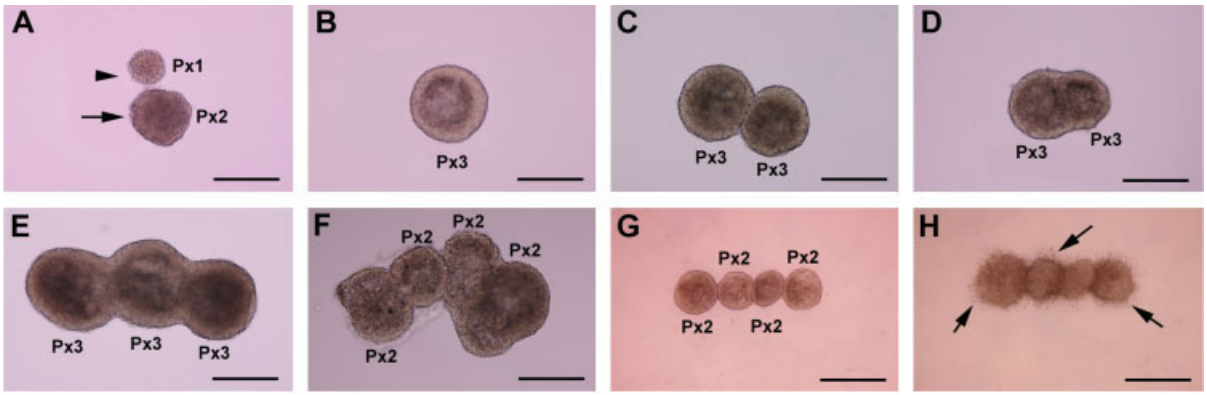

Fig. 1. Culture of proepicardial cell aggregates. Aggregation of isolated proepicardia (Px1) into complex proepicardial cell aggregates is accomplished by a suspension coculture of two (Px2) or three proepicardia (Px3). **A** illustrates a precoalescence stage; a single proepicardium (Px1, arrowhead) and an aggregate (arrow) formed by the coalescence of two proepicardia (Px2) are shown. **B** shows an aggregate formed by the coalescence of three proepicardia (Px3). **C** and **D** present two different stages in the formation of a rod-like construct developed by coalescence of two aggregates, an early attachment step (A; 2 hr of incubation) and a late coalescence stage (B; 4 hr of incubation). Note that each aggregate is formed by the coalescence of three proepicardia. **E** and **F** show rod-like constructs formed by the coalescence of three and four aggregates, respectively (for E, single aggregates are formed by the coalescence of three proepicardia, while the aggregates in F are formed by two proepicardia). **G** and **H** present the same tissue constructs (four aggregates, two proepicardia per aggregate) cultured on collagen gel. G shows the aggregates just after being transferred from the culture media to the drained gel and H after 4 hr of incubation. Arrows in H point to the diffuse border of the aggregates as the cells immigrate into the collagen gel. Scale bars = 250 μm (A–F); 500 μm (G and H).

coalesce in a round aggregate. Coalescence of two, three, or four of these aggregates to form a rod-like structure was spontaneous and usually took between 3 and 4 hr; the formed constructs ranged in length from 500 to 1,000 μm in the case of aggregates made up of two proepicardia, while those formed by three proepicardia had a total length ranging from 600 to 1,200 μm (Fig. 1D–H). Proepicardial aggregates cultured on drained collagen gels fused after 2–3 hr over the surface and initiated the invasion of the gel (Fig. 1G and H).

Scanning Electron Microscopy of Proepicardial Aggregates

The cultured proepicardial aggregates lacked the characteristic proepicardial villi, which are so conspicuous in normal proepicardia in vivo (compare Fig. 2A and B to C). As shown by SEM, the outer surface of proepicardial cell aggregates was constituted of a flattened epithelium (Fig. 2D). Suspension cultures of various cell aggregates gave rise to "pearl necklace-like" or rod-like structures (Fig. 2F–I), in which the external grooves indicating the areas of fusion were evident (Fig. 2H), although all the surface of the construct was equally covered by epithelium (Fig. 2H). Occasionally, proepicardial aggregates showed an ostium that seemed to communicate the surface with the inner core of the spheroid (Fig. 2E). Sectioning of some of the rod-like structures made evident the presence of luminal spaces inside of the tissue constructs (Fig. 2I, see also below).

Semithin Sections

Semithin sections (0.5 μm) of proepicardial aggregates confirmed the results of the SEM analysis. The outer surface of the spheroids was found to be of epithelial nature (Fig. 3A and B), while the core of the aggregates included high numbers of mesenchymal cells. The cell density was higher in the areas close to the epithelial surface than in the center of the aggregate (Fig. 3C–F). Some of these cells joined to form small tubules (Fig. 3C and D) and capillary-like structures (Fig. 3E and F).

Histological and Immunohistochemical Characterization of Proepicardial Aggregates/Spheroids: I, Cell Diversity and Coalescence of Cell Aggregates

Proepicardial aggregates express several of the characteristic markers of the epicardial tissue such as cytokeratin (CK; Fig. 4A) and retinaldehyde dehydrogenase2 (RALDH2; Fig. 4B) both in the surface and in their mesenchymal core. The quail angioblastic marker QH1 is also found in the surface and the inner compartments of the aggregates (Fig. 4A, B, E, F, and G; see also below for more details). QH1/CK or QH1/RALDH2 colocalization is frequent in these cultures (Fig. 4A and B). L-CAM (avian E-cadherin) expression was also found to occur in the surface of proepicardial aggregates, being absent from the inner mesenchymal core of the constructs. L-CAM was not present in the cells at the fusing interface of tissue constructs formed by the coalescence of two or more proepicardial aggregates (Fig. 4C).

CCFSE labeling of the epithelial surface of chick aggregates was used to develop chick-quail chimeric tissue constructs (Fig. 4D–I). CCFSE does not cross epithelial barriers and has already been used to trace transforming epithelial cells (Sun et al., 2000; Pérez-Pomares et al., 2004). The presence/absence of the dye also allowed for an analysis of proepicardial cell dynamics in vitro. Control CCFSE-labeled aggregates (cultured for 30 min) only showed the dye in the epithelial cells, which cover the surface of the aggregates (Fig. 4D). When cultured for more than 3 hr, CCFSE-labeled cells could be found in the

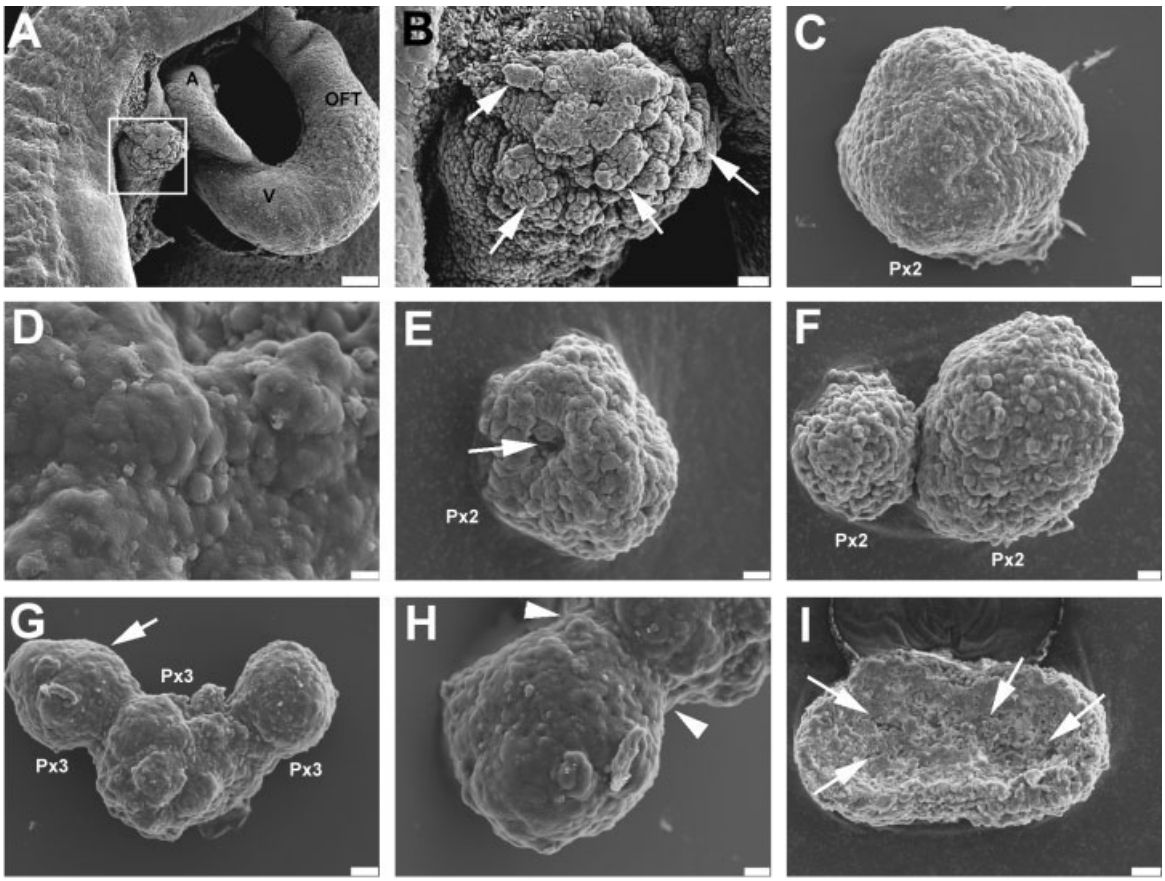

Fig. 2. Scanning electron microscopy analysis of proepicardial cell aggregates. The number of proepicardia per aggregate is indicated as in Figure 1. **A** shows the location of the proepicardium at the posterior end of the heart tube, between the sinus venosus and the liver primordium (mainly to the right side of the quail embryo). The boxed area in A is magnified in **B**. Note the rough surface of the proepicardium with its characteristic villi (arrows). **C** illustrates the external aspect of a single aggregate developed by coalescence of two proepicardia, whereas in **D**, the epithelial context of such external surface is presented. **E** shows the presence of an ostium in the surface of a different aggregate (arrow). **F–H** present different cases of coalescence of cell aggregates. In F, two aggregates of different size have coalesced, and in G, three of them form a rod-like tissue construct. The area pointed with an arrow is magnified in H to show the external side of the aggregate as well as the groove that distinctly separates fusing aggregates (arrowheads). Finally, **I** illustrates the formation of a luminal spaces (arrows) in rod-like tissue constructs (the tissue was sectioned after fixation and then imaged by SEM). Scale bars = 100 μm (A); 20 μm (B, C, G, and I); 5 μm (D); 10 μm (E, F, and H).

surface but mainly inside the aggregates (Fig. 4E–I). Coculture of quail and chick proepicardial aggregates led to their coalescence in less than 3 hr. QH1-positive cells could be found covering the quail aggregates and forming cell clusters and small endothelial tubes (Fig. 4E–G). In those tissue constructs at the very early stages of their coalescence, the QH1-positive surface of quail proepicardial aggregates made direct contact with the surface of the chick ones (Fig. 4E and F); QH1-positive cells showed projections of their cytoplasmic membrane directly attaching to the surface of chick cells (Fig. 4G). The quail panmarker QCPN was used to follow the location of quail cells at different stages of the coalescence of the chimeric constructs. During the first 3 hr, quail cells did not seem to intermingle with chick cells, and a clear border between the quail and the chick aggregates was distinct (Fig. 4H). However, after 8 or more hr of culture, quail cells could be seen crossing the border between the two proepicardial aggregates forming the construct (Fig. 4I).

Histological and Immunohistochemical Characterization of Proepicardial Aggregates/ Spheroids: II, Angioblastic/Endothelial Differentiation and Dynamic

Immunohistochemical characterization of single proepicardial cell aggregates, as well as of the tissue constructs formed by the coalescence of such aggregates, mainly focused on the differentiation of proepicardial cells into angioblasts and endothelial cells, i.e., the cell types that guide vascular formation.

Control proepicardia (cultured without growth factor supplements) did not show QH1-positive cells after 1 hr of culture (Fig. 5A). However, in the absence of VEGF and bFGF (culture control conditions: DMEM + 1% chicken serum + penicillin/streptomycin), both smooth muscle cells (after 12 hr of culture) and myocardial cells (after 48 hr in culture) differentiated in proepicardial aggregates (Fig. 5H and I). Cultures in which growth factor concen-

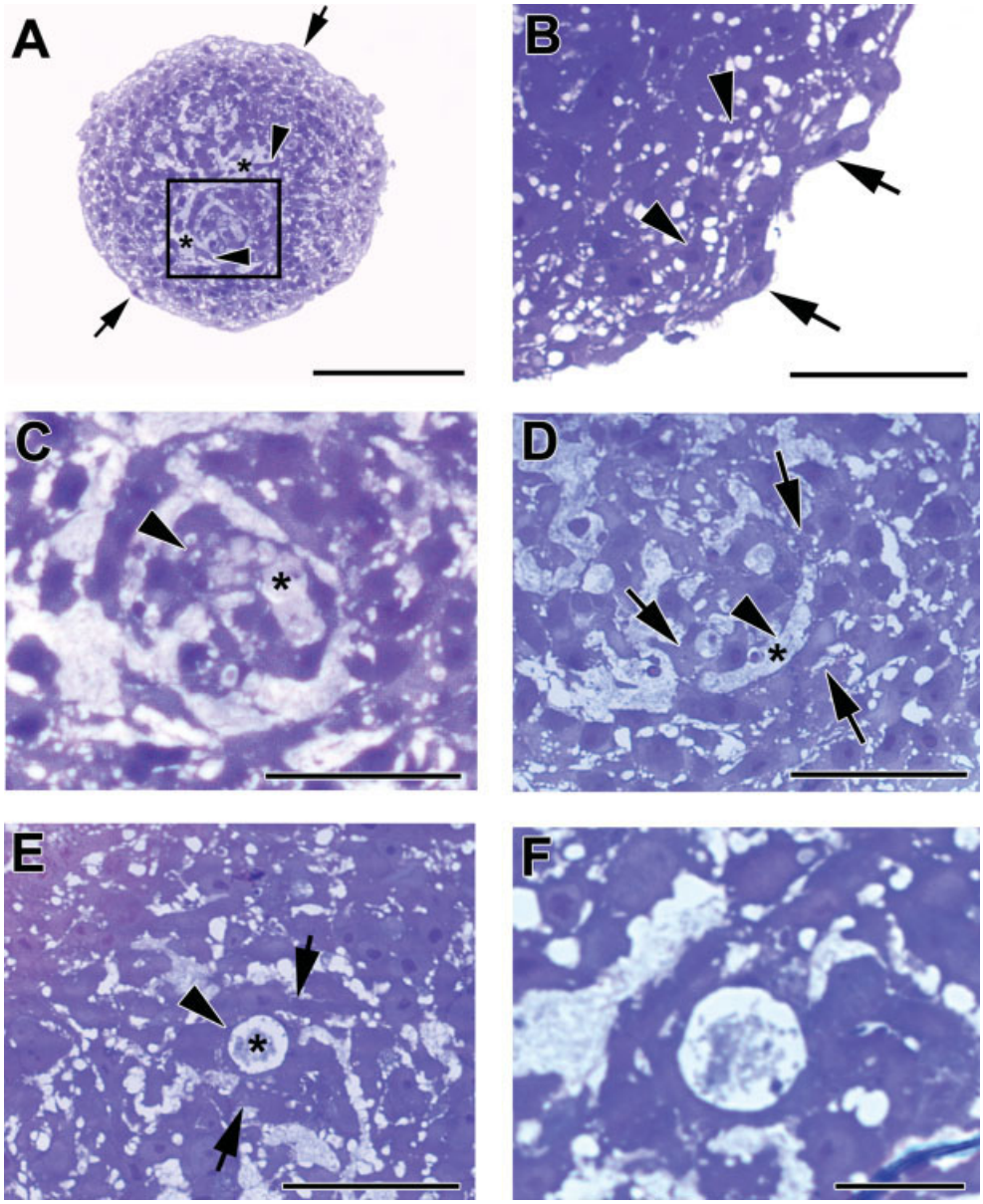

Fig. 3. Semithin sections of proepicardial cell aggregates. **A** and **B** show the general appearance of an aggregate formed by fusion of two proepicardia. A detail of the epithelial context of the surface of one of these spheroids is presented in B. The outer epithelial surface is indicated by arrows, the mesenchymal cells in the core of the aggregates are pointed by arrowheads, and the extracellular matrix marked with asterisks. The area boxed in A is magnified in **C**. The arrowhead points to a small developing vessel with a true lumen (asterisk). In **D**, a similar structure is shown in a longitudinal section (arrowhead). Note the well-developed lumen (asterisk) and the abundance of perivascular cells (arrows). A transverse section of a capillary-like structure is illustrated in **E** (arrowhead). Mesenchymal cells (arrows) surround the lumen (asterisk). **F** shows a magnification of the structure presented in E in a 1.5 μm distant section. Scale bars = 200 μm (A); 30 μm (B, D, and E); 40 μm (C); 10 μm (F).

trations lower than 100 ng/ml bFGF (not shown) and 10 ng/ml VEGF (Fig. 5D and E) were used did not present high numbers of angioblastic/endothelial cells. In no case could myocardial differentiation from proepicardial cells be recorded in the presence of bFGF and VEGF, whereas some smooth muscle differentiation was observed (not shown). Proepicardial cell aggregates cultured in the presence of growth factors (100 ng/ml bFGF; 10 ng/ml VEGF) for less than 3 hr included a very small number of QH1-positive cells, which were only found in the core of the spheroids (not shown). QH1-positive cells were mainly found in the surface as well as in the core of the aggregates in the rest of the cases studied (Fig. 5C–G and J–P). The external population of QH1-positive cells (on the surface of the aggregates) was composed of isolated cells, but also of cells forming a coherent monolayered vascular epithelium (i.e., an endothelium) that covered most of the surface of the aggregates (Fig. 5F, J, M, O, and P). However, in given

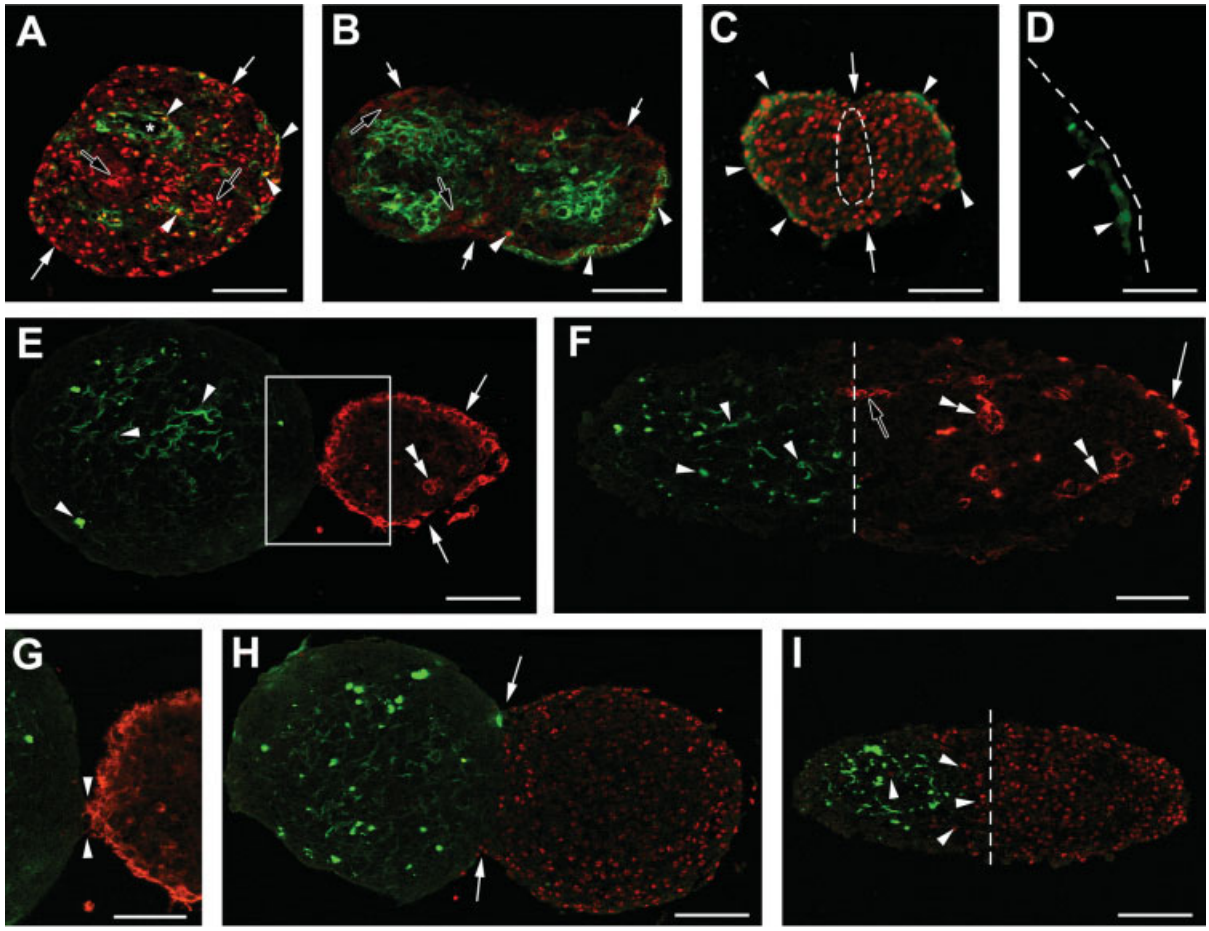

Fig. 4. Cell diversity and coalescence of cell aggregates. **A** and **B** show the expression of different epicardial markers in the proepicardial aggregates. CK (A) and RALDH2 (B) are shown in red; the proteins are found on the surface of the aggregates (white arrows) and in the mesenchymal core (black arrows). In both cases, the quail vascular marker QH1 is shown in green (note the vascular lumen in A, asterisk). Colocalization of the markers is indicated by arrowheads. **C** presents L-CAM immunoreactivity on the surface of the proepicardial aggregates (green staining, arrowheads). The grooves indicating the area of the fusion are pointed with arrows. Note the absence of L-CAM staining in the contact region between aggregates (encircled by a dashed line). **D** illustrates a control situation for CCFSE tagging. After 30 min of incubation, only some cells at the epithelial surface of the aggregates are stained (arrowheads). The external limits of the aggregate are indicated by a dashed line. **E–G** present chick-quail chimeric constructs. In E, a CCFSE-stained (green) chick aggregate initiates its fusion with a quail aggregate (its vascular cells are QH1-positive, red). Note that CCFSE-positive can be mainly found inside the aggregate (arrowheads), whereas QH1-positive cells are both on the surface (arrows) and in the core of the aggregates (double arrowheads). The area of contact (boxed) is magnified in G (a detail of the cell contact is pointed by arrowheads). In F, the coalescence between the chick and the quail aggregates is evident (the border between the quail and chick components is indicated by a dashed line). CCFSE-positive chick cells mainly remain inside the aggregate (arrowheads) while QH1-positive cells are found in the surface (arrows) and in the mesenchymal core of the tissue construct (double arrowheads). The black arrowhead points to a small vascular tube that crosses the border between the quail and chick tissues. **H** and **I** show details of the process of coalescence. All quail cell nuclei are QCPN-positive (red) and some chick cells are strongly CCFSE-stained (green). At early stages of the fusion, quail cells cannot be seen beyond the contact area between the two aggregates (arrows in H). As the fusion proceeds (I), quail cells (arrowheads) start to cross the border between the two aggregates (dashed line). Scale bars = 50 μm (A–C, E, H, and I); 40 μm (D, F, and G).

areas of these structures, more than one layer of QH1-positive cells could be seen (Fig. 5P). QH1-positive cells inside the aggregates were scattered around the hollow center and differed from the QH1-positive cells found on the outer surface of the spheroids in their diffuse QH1 immunoreactivity or their clustering into strongly QH1-positive domains (Fig. 5B–G and J–P). Finally, a certain number of the QH1-positive cells found inside the lumen of the aggregates formed small vessel-like structures, sparse or extensive endothelial linings, or true vascular tubes with a clear lumen (Fig. 5G, J–L, and N; see also Fig. 4A). All these vascular-like structures were also immunoreactive to VEGFR-2/Flk-1 antibodies (Fig. 5M and N). The local cell density found in the central region of the proepicardial aggregates was of 75 ± 5.5 cells/50 μm^2. The estimation was performed by counting propidium iodide-stained nuclei on three 20 μm-distant confocal planes per aggregate using Adobe Photoshop. QH1 immunoreactivity was used to define the percentages of vascular cells in the same standard areas and confocal planes. No evident signs of vascular morphogenesis were recorded when the percentage of vascular

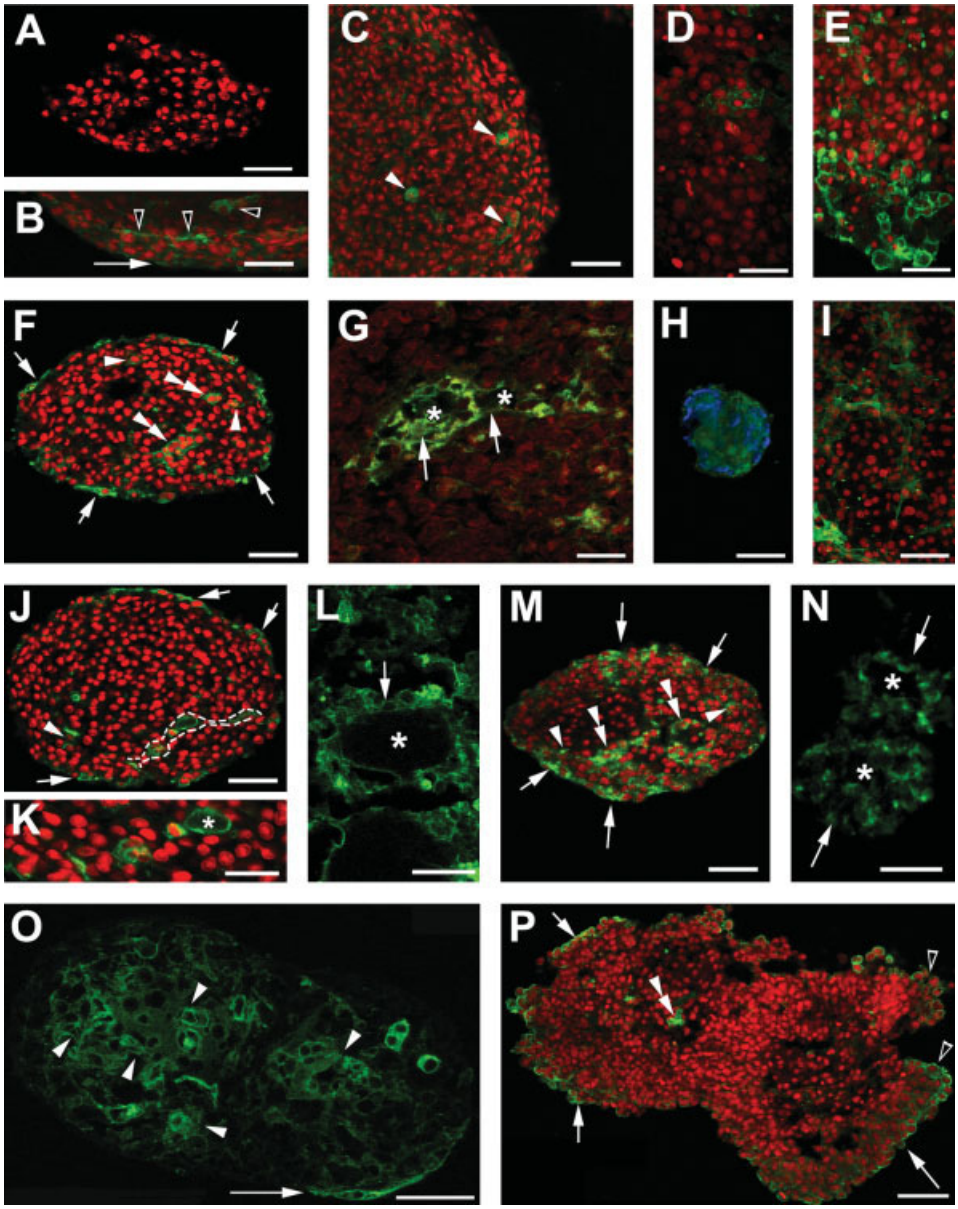

Fig. 5. Angioblastic/endothelial differentiation and dynamic. **A–G** and **J–P** show different aspects of endothelial differentiation and sorting in proepicardial aggregates and diverse tissue constructs. The green staining indicates QH1 immunoreactivity (except for M and N, where it shows VEGFR-2 expression) and the red staining is a propidium iodide nuclear counterstaining. No vascular cells (QH1-positive) can be seen in control cultured proepicardia (A), whereas myocardial cells (MF20-positive, blue staining; CK-positive, green staining) and smooth muscle cells (α-smooth muscle actin-positive, green staining; nuclear propidium iodide counterstaining, red) spontaneously differentiate in these aggregates (**H** and **I**, respectively). B and C present images from a whole-mount immunostaining of a proepicardial aggregate. Quail endothelial cells (QH1-positive, green staining) are distributed both on the surface (arrows) and inside the cell spheroids (arrowheads). In B, the formation of chords of QH1-positive cells (black arrowheads) just beneath the surface of the cell aggregate is illustrated. Aggregates treated with 5 ng/ml VEGF (D) had less angioblastic/endothelial cells (QH1-positive, in green) than cultures treated with 10 ng/ml VEGF (E). F, G, J, and K present results from the analysis of sectioned (10 μm) proepicardial aggregates. F and J: Quail endothelial cells (QH1-positive, green) appear on the surface of the spheroids as single isolated cells or forming a continuous monolayered patch of cells (arrows). Quail endothelial cells are often found inside the spheroids both isolated (arrowheads) and in clusters of different size (double arrowheads), but also forming small endothelial-lined vessel-like structures (indicated by a dashed line in J). This very same area has been magnified in K to show a detail of the vascular tube that includes a developing lumen (asterisk in K). Different vascular structures (arrows) with an evident lumen (asterisks) are presented in G and L. Similar images to those shown in F, G, J, K, and L are presented in M and N, but now the vascular marker shown by the green staining is VEGFR-2. Vascular (VEGFR-2-positive cells) are found covering the surface of the aggregate (arrows) and inside the spheroid, both as single (arrowheads) or clustered cells (double arrowheads). The magnification in N illustrates the presence of a vascular lumen (asterisk) in forming vascular structures (arrows). O and P show images from rod-like tissue constructs originated by the self-assembly of various proepicardial aggregates. QH1-positive cells can form a coherent endothelium over the surface of the aggregates (arrows in O and P), often showing a local double layering of the outer endothelial cover (black arrowheads in P). Angioblastic cells can also develop into an extensive vascular network (arrowheads in O). In some other cases (P), few cells displaying a faint QH1 immunoreactivity are found in the core of the aggregates (white arrowheads), which tend to cavitate (asterisks). Occasionally, a few groups of two or three strongly QH1-positive cells (double white arrowhead) are found inside the lumen of the aggregates. Scale bars = 60 μm (A–C, F, I, J, and M); 50 μm (D and E); 100 μm (H); 30 μm (G, K, L, and N); 40 μm (O and P).

cells (QH1-positive) in the core of the aggregates was lower than 28%.

The analysis of the rod-like tissue constructs clearly demonstrated that the outer surface of these constructs is covered by a monolayered flattened epithelium including QH1-positive endothelial domains (Fig. 5O and P). In some cases, an extensive vascularization was recorded all through the core of the aggregates (Fig. 5O). The presence of hollow spaces within the aggregates was also documented (in approximately 50% of the cases). These inner cavities often included several free mesenchymal cells (Fig. 5P) and were easily distinguishable from true developing vascular spaces, which were delineated by QH1/VEGFR-2-positive cells (Fig. 5K–O).

Apoptosis in Proepicardial Aggregates/Spheroids

To check the status of the cells that formed the aggregates, we used the TUNEL assay for in situ apoptotic cell death. All the spheroids and tissue constructs tested for apoptosis showed a few TUNEL-positive cells distributed both in their outer and inner surfaces (Fig. 6). Apoptosis was less frequent in aggregates formed after the fusion of two proepicardia than in those formed by the fusion of three (not shown). When TUNEL was combined with QH1 staining to reveal specific apoptosis in endothelial cells, it was found that only in a third of the aggregates was apoptosis basically endothelial (Fig. 6C), whereas in the rest of the cases cell death affected endothelial as well as nonendothelial cells (Fig. 6A and B).

Immunohistochemical Characterization of Myocardial-Proepicardial Chimeric Aggregates

As already indicated, quail proepicardia were aggregated and cocultured with myocardial cells to test the proepicardial potential to vascularize the myocardium in vitro. Chimeric proepicardial-myocardial aggregates formed spheroids with a diameter of about 300–450 μm (Fig. 7A). In quail proepicardial-chick myocardial aggregates, quail cells were mainly found in the outer surface of the spheroids as evidenced by QCPN staining. Some proepicardial cells, however, seemed to have migrated into the myocardial core of the aggregates (Fig. 7A and B). QH1 staining of the isolated aggregates revealed that quail angioblastic cells had invaded the aggregates, and that some of them apparently did coalesce into thin networks of capillary-like structures (Fig. 7C). Control myocardial aggregates did not show QCPN or QH1 immunoreactivity. The cells in these spheroids were completely constituted of chick myocardiocytes as revealed by specific myocardial immunostaining (Fig. 7D).

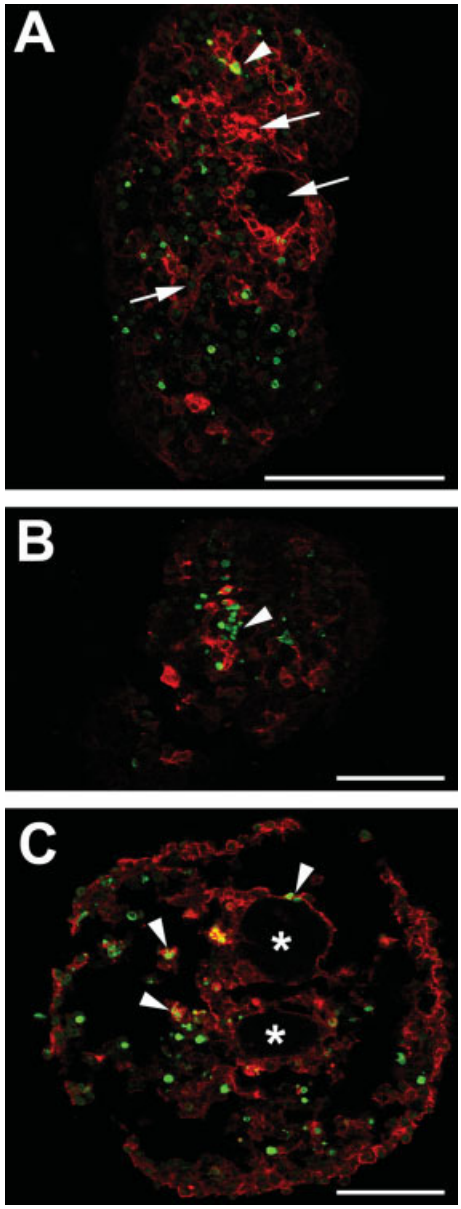

Fig. 6. Cell death in proepicardial aggregates. **A–C** show different levels and distribution of apoptosis in proepicardial aggregates. In A, scattered signs of apoptosis (green dots, arrowheads) are found in several QH1-positive cells inside vascularized spheroids. Some QH1-positive vascular networks (in red) are indicated with arrows. B illustrates the presence of apoptosis (green dots, arrowhead) in the center of an aggregate without significant association with vascular structures (QH1-positive, in red), whereas C shows evident apoptosis (green dots, arrowheads) in wide vascular-like structures (asterisks). Scale bars = 60 μm (A–C).

DISCUSSION

Epicardial progenitors (proepicardial cells) are an extremely plastic type of embryonic tissue. Actually, proepicardial cells have been proposed to be a pluripotent cell lineage; proepicardial derivatives would include coronary endothelial and smooth muscle cells, cardiac fibroblasts, and myocardium (Mikawa and Fischman, 1992; Mikawa and Gourdie, 1996; Gittenberger-de Groot et al., 1998; Pérez-Pomares et al., 1998a, 1998b, 2002a, 2002b; data not shown and this study), as well as an undifferentiated invasive population of EPDCs that is thought to constitute an embryonic pool of cardiac stem-like cells (Wessels and Pérez-Pomares, 2004). In this study, we focused on characterizing the in vitro development of endothelial vascular structures from proepicardial aggregates. Proepicardial (coronary progenitor) cells are easy to isolate and culture, and grow nicely in different in vitro assays (Guadix et al., 2006; this study). We would thus like to propose coronary cell precursors as a suitable cellular model for vascular

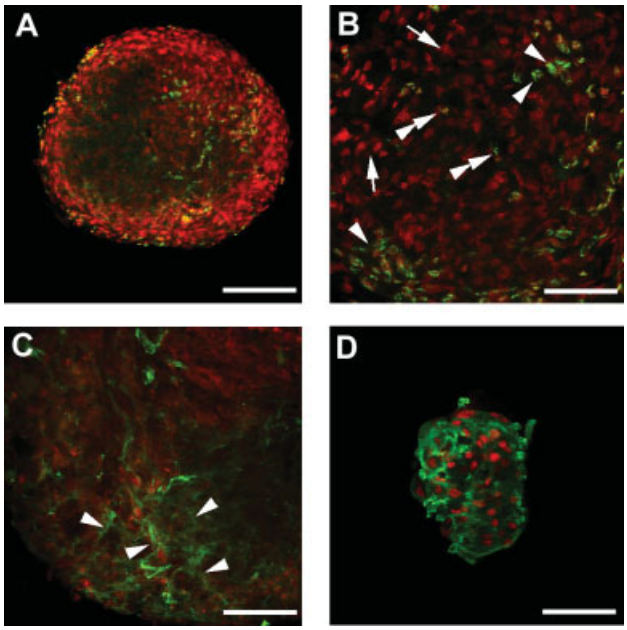

Fig. 7. Myocardial-proepicardial chimeric aggregates. **A** and **B** illustrate the results after quail proepicardial-chick myocardial cell cocultures. Quail proepicardial cells are seen as green dots among chick myocardial cells (A). Specifically, the magnification in B shows QCPN-positive cells (appearing as green domains on propidium iodide counterstained nuclei), on the surface (arrowheads), but also inside (double arrowheads) the mass of chick myocardial tissue (propidium iodide-counterstained red nuclei, arrows). In **C**, quail endothelial cells (QH1-positive, labeled in green) are shown forming capillary-like networks (arrowheads). An external control aggregate (only myocardial cells) is shown in **D**; myosin heavy chain immunoreactivity is displayed in green and cell nuclei are counterstained with propidium iodide (red). Scale bars = 120 μm (A and C); 60 μm (B and D).

tissue engineering. However, although the analysis of smooth muscle and myocardial cell differentiation from proepicardial cells/aggregates is being carried out independently from this study (data not shown), we have decided to illustrate these two differentiation events in this article to support the concept pluripotency of proepicardial cell. Smooth muscle and myocardial differentiation from proepicardial cells spontaneously occurs in culture (with no bFGF or VEGF supplements), seemingly representing the in vitro default differentiation pathway for these cells.

The suspension culture system used in this study (hanging drop) (Rudnicki and McBurney, 1987) allowed for a careful control the aggregation of different proepicardial units, avoiding the dispersion of proepicardial cells, thus helping us to study the spontaneous coalescence of cells and tissue morphogenesis on a fluidic regime. Morphologically, tissue constructs (as single proepicardial aggregates) were constituted of an external monolayered epithelium, which was continuous around their surface. Inside these structures, an inner mesenchyme containing vascular and nonvascular cells was found.

Which one is the origin of these vascular cells? It is well known that the early embryonic proepicardium (i.e., just before its attachment to the myocardial surface) is devoid of differentiated vascular cells (Kattan et al., 2004; Guadix et al., 2006). However, once the proepicardium establishes contact with the myocardium, the proepicardial tissue immediately initiates a massive differentiation into the endothelial cell lineage (Guadix et al., 2006). This myocardial instruction can be substituted in vitro by the addition of growth factors to the culture media, in this case bFGF and VEGF, two growth factors that are known to be crucial to coronary vascular morphogenesis (Risau and Flamme, 1995; Tomanek and Zheng, 2002). VEGF and bFGF are commonly provided by nonvascular neighboring tissues (e.g., the myocardium in the heart and the endoderm in the case of other viscera), but we demonstrate here that addition of bFGF (100 ng/ml) and VEGF (10 ng/ml) to the culture media partially mimics the in vivo vasculogenic triggering effect of other nonendothelial cell types, eliciting vascular differentiation and morphogenesis in the proepicardial aggregates. Several original reports have suggested that bFGF is required for proper vascular differentiation in avians but not in mammals (Risau et al., 1988; Krah et al., 1994). As indicated above, the growth factor concentrations were suggested by different studies on the differentiation of early quail embryonic mesodermal cells into angioblasts (Krah et al., 1994; Eisenberg and Markwald, 1997) as well as from preliminary unpublished results from our laboratory. Some other researchers have used different growth factor concentrations, but in different experimental systems (Cox and Poole, 2000; Tomanek et al., 2001a, 2001b). In our assay, local cell density is a critical factor, and slight variations from one proepicardial aggregate to another might influence the final concentration of angioblasts per sample. Further studies using equal amounts of cells per aggregate and testing different concentrations of growth factors from different origins (different commercial suppliers) will be necessary to define the biological provasculogenic activity of bFGF and VEGF on proepicardial cells in culture.

Culturing proepicardial tissue in hanging drop cultures clearly illustrates that cell differentiation and migration in proepicardial aggregates are coupled phenomena. As shown by our results, proepicardial aggregates strongly stain for different (pro)epicardial markers such as CK and RALDH2. The frequent colocalization of such molecules with the quail angioblastic/endothelial marker QH1 (already described in vivo by Pérez-Pomares et al., 1998a) supports the hypothesis of a direct differentiation of coronary angioblastic cells from mesothelial or mesothelial derived cells (Pérez-Pomares et al., 1998a, 1998b, 2002a, 2002b).

Previous assays performed in our laboratory indicated that single proepicardia cultured in suspension systems do not support extensive vasculogenesis, so for this study two or three proepicardia have been assembled in vitro to give rise to larger cell aggregates. Our results show that proepicardial cells grown under such conditions keep intact their ability to differentiate into endothelial cells in vitro. Formation of small endothelial-lined cavities inside the proepicardial aggregates is strongly reminiscent of in vivo vasculogenic processes. This phenomenon is usually related to the presence of high numbers of endothelial progenitors in the core of the spheroids, something that directly relates to local endothelial cell density, a critical factor modulating vasculogenic blood vessel formation (LaRue et al., 2003). In our culture system, vascular structures in proepicardial aggregates were only found when angioblastic/endothelial cells constituted approximately 30% of the total number of cells found in the center of the

cell spheroids. In this regard, it is also important to emphasize that apoptosis is a common event in proepicardial cell aggregates. The occurrence of apoptosis could explain the absence of developing vascular structures in around 30% of the sampled proepicardial aggregates, but also the massive cavitation found in other aggregates. It is conceivable that, in these cases, endothelial development could be impaired by endothelial cell apoptosis after the cells in the center of the aggregate are deprived of culture medium, as apoptosis seems to be a characteristic endothelial response to reduced levels of VEGF (Meeson et al., 1999). In this scenario, the communication of the lumen with the outer culture medium found to occur in some aggregates could be a factor minimizing endothelial apoptosis in the core of the spheroids because the described presence of these ostia can provide a sort of homeostatic perfusion to the system.

Some of the results included in this study indicate that proepicardial aggregates are able to autoregulate a seeming sorting of angioblastic/endothelial cells (QH1/VEGFR-2-positive) as they differentiate. Surprisingly, this sorting seems to be double: endothelial cells differentiating in the proepicardial aggregates migrate to the outer surface of the proepicardial tissue or to the center of the aggregate. The outer sorting can be explained by the conditions of the culture media that, as already indicated, contained bFGF and VEGF, two cytokines with chemotactic abilities that could have attracted differentiating angioblasts and supported their maturation and differentiation (Poole et al., 2001). A complementary explanation for this outer endothelial sorting can base in a difference of cohesiveness between the newly differentiated endothelial cells and the rest of the proepicardial tissue, so that if endothelial cells have a lower surface tension than other nonendothelial proepicardial cells, the former population will distribute on the outer surface of the aggregate (Foty et al., 1996). However, it is important to emphasize that this concept only applies for true cell phases, which means that a sufficient number of cells of each type is needed for adhesion-based sorting to take place. Under this assumption, the presence of angioblasts in the core of the aggregates can be interpreted as the result of the trapping of some of these cells that, unable to associate with other angioblasts, could not sort out. However, an active sorting to the internal side of the aggregates (evidenced by the dynamics of QH1-positive cells and the tracing of CCFSE-stained mesothelial cells from the outer surface of the aggregates) can also be explained by the matrix requirements of these cells, which need a well-developed 3D ECM to undergo vascular morphogenesis (Ingber and Folkman, 1989; Risau and Flamme, 1995). This relates with the finding that vascular-like structures in the proepicardial aggregates, including small endothelial tubes, are only found in the core of the spheroids. Interestingly, in this study, proepicardial tissue has been shown to be able to vascularize the embryonic myocardium in vitro, as it does in vivo (Mikawa and Fischman, 1992; Pérez-Pomares et al., 1998a, 2002a, 2004; Männer, 1999). These results strongly support the idea that a main potential of proepicardial cells is a vascular one.

In addition to reporting the differentiation of angioblastic/endothelial cells from proepicardial tissue in vitro, in this work we have also shown that proepicardial cells are a good model to study tissue self-assembly or tissue fusion, a process that could be very useful for tissue engineering procedures, specifically for vascular tissue engineering. In recent years, tissue engineering has become a more dynamic science; cell distribution and arrangement on a synthetic or biological scaffold was thought to be a passive cell-dependent variable of in vitro culture systems. Tissue engineering has shifted to a more active control of cell seeding into the substrate, an approach conceptually enhanced by the evolution and improvement of microarray printers (Delehanty and Ligler, 2003). Deposition of proteins to develop a 3D structure by superimposition of 2D layers (Rapid Prototyping Technology) (Cooper, 2001) has been essential in providing the conceptual frame on which tissue/organ printing, a new branch of tissue engineering, is based (Wilson and Boland, 2003).

Our results show that cocultured proepicardia spontaneously undergo self-assembly to form cell spheroids. In turn, several of these aggregates or spheroids can be cultured together again to form elongated rod-like or pearl necklace-like tissue constructs. The coalescence of proepicardial aggregates is a relatively quick event (3–4 hr) in both suspension and collagen gel cultures, a result that points to a cell-to-cell adhesion mechanism as the eliciting force of such fusion. Cadherins are very likely to be involved in this process. E-cadherin is actually expressed by epicardial cells (Wada et al., 2001) and just because cadherins display homophilic adhesion properties (Kemler, 1992), it is reasonable to accept that these molecules are involved in the fusion of mesothelial linings. The expression of L-CAM (avian E-cadherin) by an important part of the cells at the surface of the aggregates and its clear downregulation at the junction of coalescing proepicardial aggregates is a strong evidence for true tissue fusion. In some cases, significant numbers of vascular cells can be found at the surface of the cell spheroids; as vascular cells express their own type of cadherin (VE-cadherin) (Lampugnani et al., 1995; Vittet et al., 1997), these cells could also lead the fusion of different proepicardial constructs as suggested by our results. An additional evidence that points to a real fusion of tissues (rather than to a passive contact of different cells masses) is the real mixing of cells from the coalescing units as the assembly of the tissue proceeds (Fig. 4). This fusion event is in accordance with theories on embryonic tissue fluidity (Foty et al., 1994; Forgacs et al., 1998), specifically the differential adhesion hypothesis (DAH), which states that cell sorting is regulated by the differential cohesivity of the tissue phases (Steinberg, 1962a, 1962b, 1963, 1970, 1975; Foty et al., 1996; Steinberg and Foty, 1997; Foty and Steinberg, 2005).

As a final result of the self-assembly of partially vascularized aggregates, the resulting tissue constructs also tend to fuse their vascular cavities. This hanging drop culture setting opens a chance for experimentation with these or other pluripotent cells when cultured on thermosensitive gels (i.e., originally fluid matrices that turn to a semisolid/gel conformation after changing the temperature) (Boland et al., 2003). Self-assembly of vascularized aggregates to drive vascular cavitation in rod-like structures is a unique in vitro assay for vasculogenesis (specifically for those late aspects related to endothelial fusion) (Drake and Little, 1999), as well as a candidate technology to create vessels of variable size in vitro for their use in regenerative medicine.

ACKNOWLEDGMENTS

The QH1, QCPN, MF20, and 7D6 (L-CAM) monoclonal antibodies were obtained from the Developmental Studies Hybridoma Bank maintained by the Department of Pharmacology and Molecular Sciences, John Hopkins University School of Medicine, Baltimore, Maryland, and the Department of Biological Sciences, University of Iowa, Iowa City, Iowa, under contract NO1-HD-2-3144 from the NICHD. The L53 polyclonal and the 5H6 monoclonal antibodies were kind gifts from Professor A.F.M. Moorman (AMC-University of Amsterdam, Amsterdam, The Netherlands) and Dr. A. Eichmann (Institute de Biologie Paris-CNRS, Paris, France), respectively. The anti-RALDH2 polyclonal was a kind gift from Dr. Peter McCaffery and Dr. Ursula Dräger (Eunice Kennedy Shriver Center-UMASS). The authors thank G. Martín for his kind help in operating the scanning electron microscope and M. González-Iriarte for his expert advice on the use of the TUNEL assay. Supported by Ministerio de Sanidad y Consumo grant PIO31159 (to J.M.P.-P. and R.M.-C.); Ministerio de Ciencia y Tecnología grant BFU2005-00483 (to R.M.-C. and J.M.P.-P.); North Atlantic Treaty Organization grant LST.CLG 980429 (to J.M.P.-P.); and European Union grant LSHM-2005-018630 (to J.M.P.-P. and R.M.-C.).

LITERATURE CITED

Armstrong MT, Lee DY, Armstrong PB. 2000. Regulation of proliferation of the fetal myocardium. Dev Dyn 219:226–236.

Armstrong MT, Armstrong PB. 2003. Growth factor modulation of the extracellular matrix. Exp Cell Res 288:235–245.

Boland T, Mironov V, Gutowska A, Roth EA, Markwald RR. 2003. Cell and organ printing 2: fusion of cell aggregates in three-dimensional gels. Anat Rec 272A:497–502.

Cooper KG. 2001. Rapid prototyping technology: selection and application. New York: Marcel Dekker.

Cox CM, Poole TJ. 2000. Angioblast differentiation is influenced by the local environment: FGF-2 induces angioblasts and patterns vessel formation in the quail embryo. Dev Dyn 218:371–382.

De la Pompa JL, Zeller R. 1993. Ectopic expression of genes during chicken limb pattern formation using replication defective retroviral vectors. Mech Dev 43:187–198.

Delehanty JB, Ligler FS. 2003. Method for printing functional protein microarrays. Biotechniques 34:380–385.

Drake CJ, Little CD. 1999. VEGF and vascular fusion: implications for normal and pathological vessels. J Histochem Cytochem 47: 1351–1356.

Eisenberg CA, Markwald RR. 1997. Mixed cultures of avian blastoderm cells and the quail mesoderm cell line QCE-6 provide evidence for the pluripotentiality of early mesoderm. Dev Biol 191:167–181.

Forgacs G, Foty RA, Shafrir Y, Steinberg MS. 1998. Viscoelastic properties of living embryonic tissues: a quantitative study. Biophys J 74:2227–2234.

Foty RA, Forgacs G, Pfleger CM, Steinberg MS. 1994. Liquid properties of embryonic tissues: measurement of interfacial tensions. Phys Rev Lett 72:2298–2301.

Foty RA, Pfleger CM, Forgacs G, Steinberg MS. 1996. Surface tensions of embryonic tissues predict their mutual envelopment behavior. Development 122:1611–1620.

Foty RA, Steinberg M. 2005. The differential adhesion hypothesis: a direct evaluation. Dev Biol 278:255–263.

Gittenberger-de Groot AC, Vrancken Peeters MP, Mentink MM, Gourdie RG, Poelmann RE. 1998. Epicardium-derived cells contribute a novel population to the myocardial wall and the atrioventricular cushions. Circ Res 82:1043–1052.

González-Crussi F. 1971. Vasculogenesis in the chick embryo. An ultrastructural study. Am J Anat 130:441–460.

Guadix JA, Carmona R, Muñoz-Chápuli R, Pérez-Pomares JM. 2006. In vivo and in vitro analysis of the vasculogenic potential of avian proepicardial and epicardial cells. Dev Dyn 235:1014–1026.

Hamburger V, Hamilton HL. 1951. A series of normal stages in the development of the chick embryo. J Morphol 88:49–92.

Hertig AT. 1935. Angiogenesis in the early human chorion and in the primary placenta of the macaque monkey. Contrib Embryol Carnegie Inst 25:37–81.

Hogan BL, Kolodziej PA. 2002. Organogenesis: molecular mechanisms of tubulogenesis. Nat Rev Genet 3:513–523.

Ingber DE, Folkman J. 1989. How does extracellular matrix control capillary morphogenesis? Cell 58:803–805.

Kattan J, Dettman RW, Bristow J. 2004. Formation and remodeling of the coronary vascular bed in the embryonic avian heart. Dev Dyn 230:34–43.

Kemler R. 1992. Classic cadherins. Semin Cell Biol 3:149–155.

Krah K, Mironov V, Risau W, Flamme I. 1994. Induction of vasculogenesis in quail blastodisc-derived embryoid bodies. Dev Biol 164: 123–132.

Lalan S, Pomerantseva I, Vacanti JP. 2001. Tissue engineering and its potential impact on surgery. World J Surg 25:1458–1466.

Lampugnani MG, Corada M, Caveda L, Breviario F, Ayalon O, Geiger B, Dejana E. 1995. The molecular organization of endothelial cell to cell junctions: differential association of plakoglobin, beta-catenin, and alpha-catenin with vascular endothelial cadherin (VE-cadherin). J Cell Biol 129:203–217.

Langer R, Vacanti JP. 1993. Tissue engineering. Science 260:920–926.

Lanza RP, Langer R, Vacanti J. 2000. Principles of tissue engineering. San Diego, CA: Academic Press.

LaRue AC, Mironov V, Argraves WS, Czirok A, Fleming PA, Drake CJ. 2003. Patterning of embryonic blood vessels. Dev Dyn 228:21–29.

Männer J. 1999. Does the subepicardial mesenchyme contribute myocardioblasts to the myocardium of the chick embryo heart? a quail-chick chimera study tracing the fate of the epicardial primordium. Anat Rec 255:212–226.

Männer J, Pérez-Pomares JM, Macías D, Muñoz-Chápuli R. 2001. The origin, formation and developmental significance of the epicardium: a review. Cell Tissues Organs 169:89–103.

Meeson AP, Argilla M, Ko K, Witte L, Lang RA. 1999. VEGF deprivation-induced apoptosis is a component of programmed capillary regression. Development 126:1407–1415.

Mikawa T, Fischman, DA. 1992. Retroviral analysis of cardiac morphogenesis: discontinuous formation of coronary vessels. Proc Natl Acad Sci USA 89:9504–9508.

Mikawa T, Gourdie RG. 1996. Pericardial mesoderm generates a population of smooth muscle cells migrating into the heart along with ingrowth of the epicardial organ. Dev Biol 174:221–232.

Mironov V, Boland T, Trusk T, Forgacs G, Markwald RR. 2003. Organ printing: computer-aided jet-based 3D tissue engineering. Trends Biotechnol 21:157–161.

Nerem RM, Sambanis A. 1995. Tissue engineering: from biology to biological substitutes. Tissue Eng 1:3–13.

Pérez-Pomares JM, Macías D, García-Garrido L, Muñoz-Chápuli R. 1998a. The origin of the subepicardial mesenchyme in the avian embryo: an immunohistochemical and quail-chimera study. Dev Biol 200:57–68.

Pérez-Pomares JM, Macías D, García-Garrido L, Muñoz-Chápuli R. 1998b. Immunolocalization of the vascular endothelial growth factor receptor-2 in the subepicardial mesenchyme of hamster embryos: identification of the coronary vessel precursors. Histochem J 30:627–634.

Pérez-Pomares JM, Carmona R, González-Iriarte M, Atencia G, Wessels A, Muñoz-Chápuli R. 2002a. Origin of coronary endothelial cells from epicardial mesothelium in avian embryos. Int J Dev Biol 46:1005–1013.

Pérez-Pomares JM, Phelps A, Sedmerova M, Carmona R, González-Iriarte M, Muñoz-Chápuli R, Wessels A. 2002b. Experimental studies on the spatiotemporal expression of WT1 and RALDH2 in the embryonic avian heart: a model for the regulation of myocardial and

valvuloseptal development by epicardially-derived cells (EPDCs). Dev Biol 247:307–326.
Pérez-Pomares JM, Carmona R, González-Iriarte M, Macías D, Guadix JA, Muñoz-Chápuli R. 2004. Contribution of mesothelium-derived cells to liver sinusoids in avian embryos. Dev Dyn 229:465–474.
Poole TJ, Finkelstein EB, Cox CM. 2001. The role of FGF and VEGF in angioblast induction and migration during vascular development. Dev Dyn 220:1–17.
Risau W, Lemmon V. 1988. Changes in the vascular extracellular matrix during embryonic vasculogenesis and angiogenesis. Dev Biol 125:441–450.
Risau W, Sariola H, Zerwes HG, Sasse J, Ekblom P, Kemler P, Doetschmann T. 1988. Vasculogenesis and angiogenesis in embryonic-stem-cell-derived embryoid bodies. Development 102:471–478.
Risau W, Flamme I. 1995. Vasculogenesis. Annu Rev Cell Dev Biol 11:73–91.
Rudnicki MA, McBurney MW. 1987. Cell culture methods and introduction of differentiation of embryonal carcinoma cell lines. In: Robertson EJ, editor. Teratocarcinomas and embryonic stem cells: a practical approach. Oxford: IRL Press. p 19–49.
Steinberg MS. 1962a. Mechanism of tissue reconstruction by dissociated cells: II, time-course of events. Science 137:762–763.
Steinberg MS. 1962b. On the mechanism of tissue reconstruction by dissociated cells: I, population kinetics, differential adhesiveness. and the absence of directed migration. Proc Natl Acad Sci USA 48:1577–1582.
Steinberg MS. 1963. Reconstruction of tissues by dissociated cells: some morphogenetic tissue movements and the sorting out of embryonic cells may have a common explanation. Science 141:401–408.
Steinberg MS. 1970. Does differential adhesion govern self-assembly processes in histogenesis? Equilibrium configurations and the emergence of a hierarchy among populations of embryonic cells. J Exp Zool 173:395–433.
Steinberg MS. 1975. Adhesion-guided multicellular assembly: a commentary upon the postulates, real and imagined, of the differential adhesion hypothesis, with special attention to computer simulations of cell sorting. J Theor Biol 55:431–443.
Steinberg MS, Foty RA. 1997. Intercellular adhesions as determinants of tissue assembly and malignant invasion. J Cell Physiol 173:135–139.
Sun D, Griffith CM, Hay ED. 2000. Carboxyfluorescein as a marker at both light and electron microscope levels to follow cell lineage in the embryo. In: Tuan RS, Lo CW, editors. Developmental biology protocols, vol. 1. Totowa, NJ: Humana Press. p 357–363.
Tomanek RJ, Ratajska A, Kitten GT, Yue X, Sandra A. 1999. Vascular endothelial growth factor expression coincides with coronary vasculogenesis and angiogenesis. Dev Dyn 215:54–61.
Tomanek RJ, Sandra A, Zheng W, Brock T, Bjercke RJ, Holifield JS. 2001a. Vascular endothelial growth factor and basic fibroblast growth factor differentially modulate early postnatal coronary angiogenesis. Circ Res Jun 88:1135–1141.
Tomanek RJ, Zheng W, Peters KG, Lin P, Holifield JS, Suvarna PR. 2001b. Multiple growth factors regulate coronary embryonic vasculogenesis. Dev Dyn 221:265–273.
Tomanek RJ, Zheng W. 2002. Role of growth factors in coronary morphogenesis. Tex Heart Inst 29:250–254.
Vacanti JP, Langer R. 1999. Tissue engineering: the design and fabrication of living replacement devices for surgical reconstruction and transplantation. Lancet 354:SI32–SI34.
Vittet D, Buchou T, Schweitzer A, Dejana E, Huber P. 1997. Targeted null-mutation in the vascular endothelial-cadherin gene impairs the organization of vascular-like structures in embryoid bodies. Proc Natl Acad Sci USA 94:6273–6278.
Vrancken Peeters MP, Gittenberger-de Groot AC, Mentink MM, Hungerford JE, Little CD, Poelmann RE. 1997a. Differences in development of coronary arteries and veins. Cardiovasc Res 36:101–110.
Vrancken Peeters MP, Gittenberger-de Groot AC, Mentink MM, Hungerford JE, Little CD, Poelmann RE. 1997b. The development of the coronary vessels and their differentiation into arteries and veins in the embryonic quail heart. Dev Dyn 208:338–348.
Vrancken Peeters MPFM, Gittenberger-de Groot AC, Mentink MMT, Poelmann RE. 1999. Smooth muscle cells and fibroblasts of the coronary arteries derive from epithelial-mesenchymal transformation of the epicardium. Anat Embryol 199:367–378.
Wada AM, Reese DE, Bader DM. 2001. Bves: prototype of a new class of cell adhesion molecules expressed during coronary artery development. Development 128:2085–2093.
Wessels A, Pérez-Pomares JM. 2004. The epicardium and epicardially derived cells (EPDCs) as cardiac stem cells. Anat Rec 276A:43–57.
Wilson C, Boland T. 2003. Cell and organ printing 1: protein and cell printers. Anat Rec 272A:492–497.